Clays and Clay Minerals, Vol. 45, No. 2, 170–183, 1997.

REFINED RELATIONSHIPS BETWEEN CHEMICAL COMPOSITION OF DIOCTAHEDRAL FINE-GRAINED MICACEOUS MINERALS AND THEIR INFRARED SPECTRA WITHIN THE OH STRETCHING REGION. PART II: THE MAIN FACTORS AFFECTING OH VIBRATIONS AND QUANTITATIVE ANALYSIS

G. BESSON[1] AND V. A. DRITS[2]

[1] CRMD-CNRS-Université, B.P. 6759, 45067 Orleans Cedex 2, France

[2] Geological Institute of the Russian Academy of Sciences, Pyzhevsky Street 7, 109017 Moscow, Russia

Abstract—A new model for the interpretation of dioctahedral mica infrared (IR) spectra in the OH stretching vibration region is proposed. It is based on the analysis of the main factors responsible for the observed sequence of the OH frequencies. In terms of this model, the simple analytical dependence between the OH frequencies and the mass and valency of cations bonded to OH groups has been found. The specific character of the interaction between octahedral Al and OH groups in the mica structures is assumed.

Integrated optical densities of the OH bands determined by the decomposition of the studied mica IR spectra are used for the quantitative analysis, that is, for the determination of a number of each type of octahedral cations per unit cell of the sample under study. A good agreement between the octahedral cation contents of 2:1 layers found from the IR spectra decomposition and the chemical analysis has shown that this technique may be used to study the local order-disorder of isomorphous cation distribution in mica structures.

The essential result obtained by the quantitative analysis of the mica IR spectra is the determination of Fe^{3+} cations in the tetrahedral sites of some samples. This means that the conventional presentation of structural formulae for Al-Fe^{3+}-containing 2:1 layer silicates is unacceptable without consideration of tetrahedral Fe^{3+} by spectroscopic techniques and by the quantitative analysis of the IR spectra, in particular.

Key Words—Cation Mass, Cation Valency, IR Spectra, OH Stretching Frequencies, Quantitative Analysis.

INTRODUCTION

In Part I of this paper, the IR spectra of a large collection of clay-size dioctahedral potassic micaceous minerals, differing in their chemical compositions, were studied (Besson and Drits 1997). Decomposition of the IR spectra has provided unambiguous identification of the band positions corresponding to each defined cation pair bonded to OH groups. A set of the empirical relationships between wavenumbers of the bands corresponding to the pairs of cations having different valency and mass has been found. The technique of IR spectra treatment has revealed for the first time the presence of pyrophyllite-like local structural environments in samples having a deficiency of K.

One of the aims of this paper is to consider the main factors responsible for the observed relationships between the OH frequencies and the definite cations bonded to OH groups. In particular, we will consider the advantages and limitations of the models described in the literature for the interpretation of the mica OH stretching vibration region, and propose a new one.

Another aim is to determine octahedral cation contents in 2:1 layers by the quantitative analysis of the IR spectra in order to provide a basis for investigation of local order-disorder in the isomorphous cation distribution. Data obtained may be useful for the study of crystal chemical features of micas. One of the problems that is not completely solved relates to the determination of tetrahedral cation content in Fe-containing clay minerals. Most researchers believed that Al has an absolute preference over Fe^{3+} for tetrahedral sites, and for this reason, only Al substitutes for Si in the tetrahedral sheets of 2:1 phyllosilicates. Calculating chemical formulae, they assign all Si presented in a chemical analysis to tetrahedral sites, and then add Al cations necessary to fill the "vacant" tetrahedral positions. The possible tetrahedral substitution of Fe^{3+} was not taken into consideration.

Theoretical considerations show that, for many structures, Fe^{3+} apparently has a preference over Al^{3+} for tetrahedral sites, whereas Al has a preference over Fe^{3+} for octahedral sites (Cardile 1989). Some tetrahedral Fe^{3+} substitution in Al-Fe containing 2:1 layer silicates should therefore exist. This assumption is supported by spectroscopic techniques (Slonimskaya et al. 1986; Johnston and Cardile 1987; Cardile and Brown 1988). For this reason, a presentation of chemical formulae is acceptable only if a possible presence

Table 1. Correlation between the mean values of the OH stretching frequencies and the octahedral cations bonded to OH groups.

Pairs	Wave number cm^{-1} Exp	Cal
Mica like		
Fe^{2+} Fe^{2+}	3505	3504.8
Fe^{2+} Fe^{3+}	3521	3519.8
Fe^{3+} Fe^{3+}	3535	3534.8
Mg Fe^{2+}	3543	3543.8
Mg Fe^{3+}		3558.8
Al Fe^{2+}	3559	3560.4
Al Fe^{3+}	3573	3575.4
Mg Mg	3583	3582.9
Al Mg	3604	3602.1
Al Al	3621	3621.3
Al Al	3641	3641.1
Al Al	3658	3658.2
Pyr. like		
Fe^{3+} Fe^{3+}	3631	
Al Fe^{3+}	3652	
Al Al	3675	

of tetrahedral Fe^{3+} was analyzed. One of the solutions to this problem is a comparison between octahedral cation content determined by the IR technique with the total cation content of a sample under study calculated from a chemical analysis.

The chemical compositions of the samples under study and the wave numbers of the OH bands corresponding to different cations bonded to OH groups were given in Part I (Besson and Drits 1997). Mean values of the frequencies, as well as the integrated optical densities of the bands corresponding to each cation pair of the samples under study, are given in Tables 1 and 2.

MAIN FACTORS RESPONSIBLE FOR THE OBSERVED CORRELATION BETWEEN OH STRETCHING FREQUENCIES AND NATURE OF CATION PAIRS BONDED TO OH GROUPS

Some Mica Structural Features and Symbolic Notations

In order to elucidate the relationship between OH stretching band intensities and frequencies as a function of composition and structure, the local structural environment around OH groups within mica 2:1 layers should be considered. In dioctahedral mica structures, each OH-group belongs to 2 *cis*-octahedra, *M2*, occupied by cations and to a vacant *M1* octahedron (Figure 1). The OH vector in such an environment is inclined to the *ab* plane towards the vacant octahedron. The ρ angle between the (001) plane and the OH-vector depends upon mica chemical composition (Giese 1979; Bookin and Drits 1982). Transition from muscovite, $K(Si_3Al_1)Al_2O_{10}(OH)_2$, to leucophyllite, $KSi_4AlMgO_{10}(OH)_2$, and celadonite, $KSi_4Fe^{3+}MgO_{10}(OH)_2$, accompanying a sequential increase of cation charge in the tetrahedral sheets and a decrease of positive charge in the octahedral sheets of 2:1 layers, is demonstrative in this respect. In muscovite, the OH-vector is oriented towards the vacant *M1* octahedron at ρ angle of 15° to the (001) plane, whereas in phengite $2M_1$, the protons are moved toward the plane of the oxygens of the octahedra (ρ = 1°) in response to the increase of the tetrahedral positive charge. The extreme case of charge distribution occurs in celadonite, where tetrahedral cations have the highest charges and octahedral cations the lowest. The protons of the 2 OH groups lie inside the *trans*-octahedron, acting as a divalent octahedral cation. The inclination of the OH vector towards the vacant *M1* octahedron decreases the distances between the proton of the OH group and the 2 nearest O_3 oxygen atoms which are of the *M1* octahedron and 2 successive (Si, Al)-tetrahedra (Figure 1). For this reason, hydrogen bonds O-H ... O_3 are formed in dioctahedral micas. The existence of such hydrogen bonds was established by the IR studies (Saksena 1964; Farmer 1974; Langer et al. 1981), as well as by the structural refinements of these minerals (Bookin and Smoliar 1985; Smoliar and Drits 1990).

The local cation environments around the OH group and the O_3 and O_1 oxygen atoms nearest to the OH group in dioctahedral mica can be symbolized as:

around OH group	around O_3 or O_1 atoms
$(M_2M_{2'})$ (Si, Si)[K]	$(M_2M_{2'})$ [Si][K]
or	or
$(M_2M_{2'})$ (Si, Al^{IV})[K]	$(M_2M_{2'})$ [Al^{IV}][K] [1]

where M_2 and $M_{2'}$ correspond to cations occuping M_2 and $M_{2'}$ *cis*-octahedra, and where each O_3 or O_1 atom is connected with Si or Al^{IV} (Figure 1).

The Vedder (1964) Model

The OH-stretching frequency, ν_{OH}, depends on the O-H bond strength, K_{OH}, and the reduced mass of the vibration system, μ_{OH}, as given by:

$$\nu_{OH} = \frac{1}{2\pi}\sqrt{\frac{K_{OH}}{\mu_{OH}}} \quad [2]$$

The K_{OH} value depends on the valency of cations bonded to OH groups, since a decrease of their common charge should lead to a strengthening of the bonding between oxygen and the proton within the OH group. For this reason, the correlation of the bands according to different OH cation neighbors, as proposed by Vedder (1964) was for a long time commonly adopted. According to this scheme, the OH stretching frequencies should decrease with an increase in the sum of valencies of the corresponding cation pair. In particular, he proposed the sequence:

https://doi.org/10.1346/CCMN.1997.0450205 Published online by Cambridge University Press

Table 2. Integrated optical densities of the OH bands corresponding to the specific cation pairs bonded to the OH groups determined by the decomposition of the IR spectra of the samples under study.

Sample	933	132	1040	Z1	69	5/1	655	TAH	PIL	68/69	E8/2
Mica like											
Fe^{2+} Fe^{2+}	4.32	1.61	0.81	6.63	5.53	1.05	2.14	5.89			
Fe^{2+} Fe^{3+}	18.81	6.27	14.52	10.43	25.80	2.79	8.10	3.92	19.65	19.01	5.29
Fe^{3+} Fe^{3+}	22.39	30.76	25.71	13.65	16.03	28.15	30.42	20.92	15.52	18.12	14.03
Mg Fe^{2+}				3.61	1.57	2.39	2.23		0.65		4.31
Mg Fe^{3+}			8.00								
Al Fe^{2+}	35.57	36.71	13.87	56.06	32.45	29.47	27.71	34.05	16.21	18.73	13.32
Al Fe^{3+}	3.45		4.95	2.57	5.56	7.76		3.94	17.32	17.49	10.18
Mg Mg	8.46	8.00	10.45	3.84	4.40	3.84	13.44	11.49	6.04	4.77	7.34
Al Mg		4.48	4.67	2.47	2.41	8.87	6.64	9.31	11.45	8.84	13.11
Al Al				0.75		2.66	6.61	6.77	7.62	8.95	9.52
Al Al								3.30	5.53	4.11	
Al Al								0.41			11.64
Pyr. like											
Fe^{3+} Fe^{3+}	6.99	12.19	17.03		6.26	13.02	2.70				11.26
Al Fe^{3+}											
Al Al											

$$M^{2+} - OH - M^{2+} \rightarrow M^{2+} - OH - M^{3+} \rightarrow M^{3+} - OH - M^{3+} \quad [3]$$
$$3625\ m^{-1} \qquad 3600\ cm^{-1} \qquad 3560\ cm^{-1}$$

However, Slonimskaya et al. (1986) noted that Vedder's interpretation does not always correspond to the observed relationship between the charge and mass of cations and the corresponding vibration frequencies. The opinion of Robert and Kodama (1988) was more categorical; they wrote that "the sequence proposed by Vedder (1964) is not true, in fact the reverse is true". Analysis of the data given in Table 1 shows that both possibilities are valid and that the appearance of the sequences is determined by the nature of cations as well as by the structural features of dioctahedral micas. The sequence proposed by Vedder (1964) is valid for combinations of Fe^{3+} and Mg cations, that is, for combinations of cations having different mass and valency. For example:

$$\nu\ (Mg\text{-}Mg) \rightarrow \nu\ (Mg\text{-}Fe^{3+}) \rightarrow \nu\ (Fe^{3+}\text{-}Fe^{3+}) \quad [4]$$
$$3583\ cm^{-1} \qquad 3559\ cm^{-1} \qquad 3535\ cm^{-1}$$

The reverse sequence is observed for Al and Mg or Fe^{3+} and Fe^{2+} cation pairs, that is, for combinations of cations having the same or similar masses:

$$\nu\ (Al\text{-}Al) \rightarrow \nu\ (Al\text{-}Mg) \rightarrow \nu\ (Mg\text{-}Mg)$$
$$3621\ cm^{-1} \qquad 3604\ cm^{-1} \qquad 3583\ cm^{-1}$$

$$\nu\ (Fe^{3+}\text{-}Fe^{3+}) \rightarrow \nu\ (Fe^{2+}\text{-}Fe^{2+}) \rightarrow \nu\ (Fe^{2+}\text{-}Fe^{2+}) \quad [5]$$
$$3535\ cm^{-1} \qquad 3521\ cm^{-1} \qquad 3505\ cm^{-1}$$

This means that, in addition to cation charge, there are other factors that control the band position for each given cation pair bonded to OH groups.

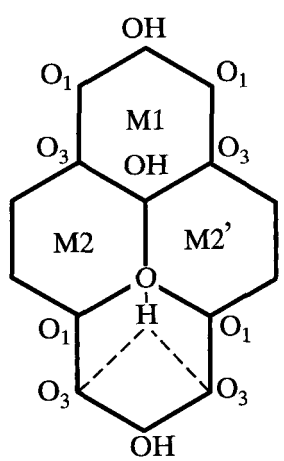

Figure 1. A fragment of the octahedral sheet of a 2:1 layer showing a local disposition of M_2 and $M_{2'}$ cations, O_1 and O_3 oxygen atoms and OH groups. M_2 and $M_{2'}$ correspond to *cis*-octahedra occupied by cations and M_1 represents a vacant *trans*-octahedron.

The Robert and Kodama (1988) Model

These authors considered correlations between the OH stretching frequencies and the compositions of micas in the system K_2O-MgO-Al_2O_3-SiO_2-H_2O, and proposed a single model for trioctahedral and dioctahedral micas. The experimental IR data for dioctahedral micas used in their paper were obtained by Velde (1978). He studied a synthetic series of micas whose compositions varied from muscovite to Al-Mg celadonite (leucophyllite) and found that there was a linear dependence between wave number of the major intensity band and the muscovite content in the solid solutions of the studied samples. Taking into account that a wave number at 3592 cm^{-1} corresponds to the Mg-Mg band, Robert and Kodama (1988) proposed the following regression:

Table 2. Extended.

40/7	CH	136	31	BP	Z2	MOL	60	RM4	RM30	38/60	BIN
				1.69							
7.35		0.26		1.06							
17.87	11.59	2.87		12.31	0.61	0.27	1.40				
2.33		3.41	1.92	0.34	0.70	0.70					
10.79	7.74	13.05	2.50	3.50	5.76		8.21				
			7.73	7.63		5.07					
6.07	27.66	4.92		2.63	0.73		3.95				
6.03	0.80	13.49	5.90	2.83	8.66	7.82	3.61				
16.70	25.82	30.24	42.20	20.68	41.47	41.76	37.51	14.75	11.27		
15.30	4.26	19.80	21.54	23.29	21.97	18.55	28.49	31.24	25.50	29.24	
9.45	17.28	4.35	2.19	13.77	7.99	19.05	13.89	19.57	30.06	26.15	
			9.43		5.31	6.77	2.93	9.50	26.81	41.30	
2.44	0.99	1.97	6.60		6.80						
2.63	3.86	4.20		10.28				8.72			4.60
3.05		1.43						16.22	6.35	3.31	95.40

$$\nu_{OH} = 11.45\ Al_t + 3592\ cm^{-1} \quad [6]$$

where $Al_t = Al^{IV} + Al^{VI}$ per unit formula. This equation should predict the position of the major intensity band in the IR spectra of tetrasilicic magnesium mica (TMM)-muscovite series.

Equation [6] shows that the transition from Al-free TMM through Al-Mg-micas to muscovite is accompanied by the successive increase of the OH stretching frequencies. Robert and Kodama (1988) supposed that the charge balance priority on apical oxygens O_3 of tetrahedra is the main factor that controls the position of the major intensity band in the OH-stretching vibration spectra. To make it more clear, let us consider the leucophyllite structural fragment consisting of octahedral cations Al and Mg, OH groups, O_3 and O_1 oxygen atoms and Si cations projected on these atoms. Figure 2 shows the local cation environments around OH groups and the oxygen atoms. The sum of the bond strengths received by the O_3 and $O_{3'}$ atoms from the nearest cations is 1.67 valent unit (v.u.) (1Si and 2Mg) and 1.833 v.u. (1Si, 1Mg and 1Al), respectively. Thus, the underbonding character of the O_3 and $O_{3'}$ atoms does not directly depend upon the type of octahedral cations bonded to the OH groups (2 Al in the case shown in Figure 2).

According to Robert and Kodama (1988), the strong underbonding of these atoms leads to the formation of relatively strong hydrogen bonds between OH and O_3, which are in turn responsible for the lowest frequency in the IR spectrum of the TMM sample. They wrote that the underbonded character of O_3 atoms is progressively reduced by the replacement of (Mg-Mg) pairs by (Mg-Al) and then by (Al-Al) pairs bonded to O_3. Therefore, the interactions OH···O_3 decrease with increasing Al content of the mica. The underbonded character of oxygen O_3 atoms is minimum in muscovite, in which all apical oxygens of the tetrahedra are bonded to $2Al^{VI}$; therefore, muscovite has the highest OH-stretching wave number. Thus, according to this model, the wave number of a band should depend mainly upon the nature of cations surrounding O_3 atoms that are responsible for the underbonded character of these anions, rather than upon the nature of the cations nearest to the OH groups.

The main consequence of the Robert and Kodama (1988) model is that different frequencies may correspond to the same nearest cation neighbors of the OH groups, and different cationic environments of the OH groups may be characterized by the same wave numbers. Such considerations relate only to the major intensity band positions and ignore the relationship between individual cation pairs nearest to OH groups and the corresponding frequencies. This conclusion is contradictory to the data obtained by Besson and Drits (1997). We have shown that, for different samples, the OH stretching frequencies corresponding to the defined cation pair are characterized by similar wave numbers and that the fluctuations in their values usually do not exceed 1–3 cm^{-1}. The presence of the resolved (Mg-Mg) band at the same position (3583 cm^{-1}) in the IR spectra of leucophyllite samples shows 1) that the absorption at 3592 cm^{-1} does not correspond to the lowest OH stretching frequency for Al-Mg containing micas, as was supposed by Robert and Kodama (1988), and 2) that the position of this band is practically independent of the underbonding character of O_3 anions, since the Mg-Mg band position varies only by $\pm$ 2 cm^{-1} in the spectra of samples having different compositions. This means that the band positions are determined first of all by the nature of the octahedral cations nearest to the OH groups and to a lesser degree by the nature of octahedral and tetrahedral cations surrounding O_3 or O_1 anions.

In terms of the model of Robert and Kodama (1988), the influence of Al^{IV} cations on the major in-

https://doi.org/10.1346/CCMN.1997.0450205 Published online by Cambridge University Press

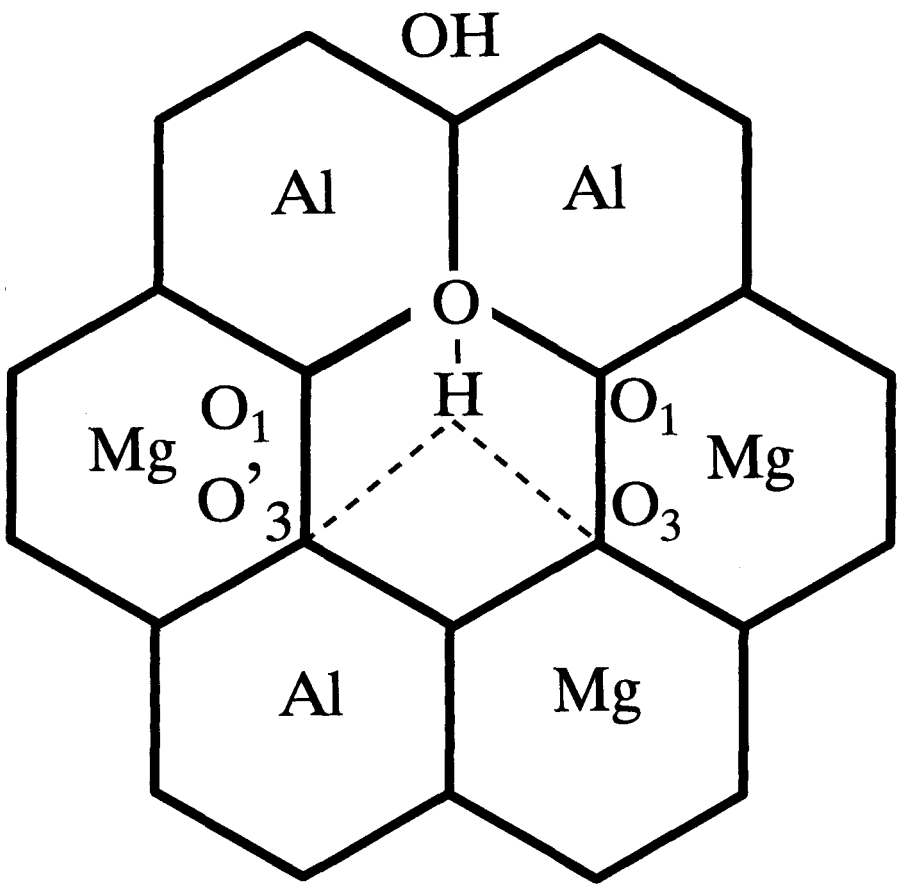

Figure 2. A fragment of the octahedral sheet of the leucophyllite 2:1 layer showing different local cation environments around O_3 atoms. Two Al cations are bonded to the OH group, which have hydrogen bonds with O_3 and $O_{3'}$ atoms.

tensity band position remains unclear. An increase in the substitution Si for Al increases the underbonded character of O_3 anions and should decrease the OH stretching frequencies. However, according to Equation [6], an increase of Al^{IV} as well as Al^{VI} should increase the OH stretching frequencies. The explanation may be very simple. Repulsion between protons and octahedral cations increases with increasing of Al^{VI}, whereas repulsion between protons and tetrahedral cations decreases with increasing of Al^{IV}. Both effects should increase the angle between OH vectors and the *ab* plane and increase the OH frequency of the major intensity band position.

It should be noted that the assumptions concerning the decisive role of the charge imbalance on the O_3 anions is not applied to the systems: K_2O-SiO_2-Fe_2O_2-MgO-H_2O or K_2O-SiO_2-Al_2O_3-MgO- Fe_2O_3-FeO.

The Proposed Model

The model we propose is based upon the assumption that the nature of cations in M_2 and $M_{2'}$ *cis*-sites is the main factor responsible for the observed sequence of the band frequencies (Table 1). The position of an individual band that corresponds to a given cation pair depends upon the sum of the bond strengths received by the OH group from the bonded octahedral cations and the mass of the cations occupying M_2 and $M_{2'}$ octahedra.

The role of the first factor has been considered in the section devoted to the Vedder model: a decrease of the total valency of cations nearest to the OH group leads to an increase of the bond strength within the hydroxyl group (as well as K_{OH}), and therefore of the corresponding frequency.

To explain the observed sequence of the band positions, it is assumed that the reduced mass of the OH stretching vibration system depends upon the mass of cations associated with the OH-group so that the frequency decreases as the mass of these cations increases. The effect of the mass of the cation pairs on the OH stretching frequencies has been formulated by Brindley and Kao (1984). These authors studied structural and IR relations among brucite-like divalent metal hydroxides. They found that, in passing sequentially from Mg to Cd hydroxide, the effective mass of the system increases, whereas the OH-stretching frequen-

https://doi.org/10.1346/CCMN.1997.0450205 Published online by Cambridge University Press

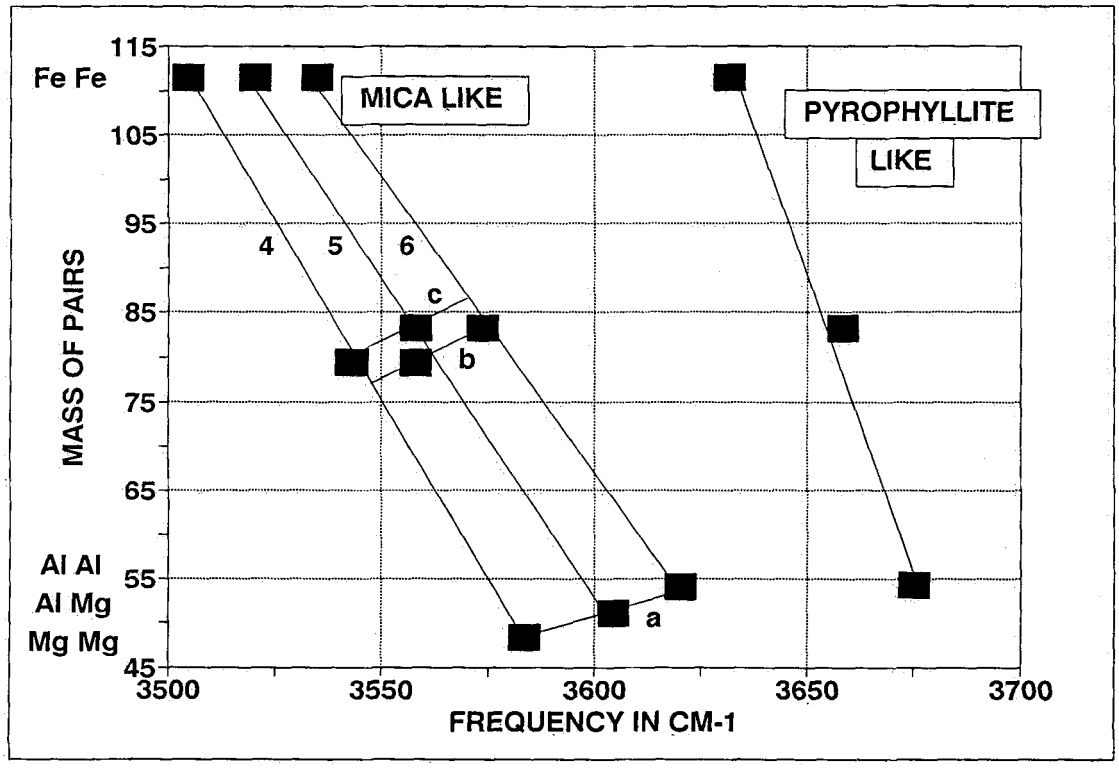

Figure 3. The relationships between the OH stretching frequencies and the mass and valency of octahedral cations bonded to OH groups. Lines 4, 5 and 6 join the values of the frequencies corresponding to the cation pairs having the sum of valencies that are equal to 4, 5 and 6, respectively. Lines a, b and c illustrate a frequency increase with increasing sum of the cation pair valencies.

cies decrease. Qualitatively, the dependence of the OH-vibration frequency upon the mass of cations associated with OH groups was also observed in the IR spectra of Mg,Ni talc (Wilkins and Ito 1967).

The relationships between the OH stretching frequencies and atomic weights for different cation pairs is shown in Figure 3. The sum of atomic weights or masses for each cation pair is plotted versus the corresponding wave number. Three lines marked as 4, 5 and 6 join the points that correspond to the cation pairs whose sums of valencies are equal to 4, 5 and 6 v.u., respectively. Each line includes 3 points and reflects the linear frequency decrease with the increasing mass of the cation pair. This dependence is observed for the Mg-Mg, Fe^{2+}-Mg, and Fe^{2+}-Fe^{2+} (line 4); Al-Mg, Fe^{3+}-Mg, and Fe^{2+}-Fe^{3+} (line 5); and Al-Al, Al-Fe^{3+}, and Fe^{3+}-Fe^{3+} bands (line 6).

On the other hand, 3 lines marked by a, b and c demonstrate the opposite effect of an increase in frequency with increasing atomic mass of the corresponding cation pairs. For example, such a tendency is observed for the sequence of points corresponding to the Mg-Mg, Mg-Al and Al-Al pairs (line a). In this case, 2 opposite tendencies overlap: the increase of mass decreases the frequency, but the simultaneous increase in the total cation valency increases the frequency. Predominance of the last factor provides the observed effect. Increase of the frequencies with the increasing of the total valency is demonstrated in Fe-Fe pairs (Figure 3).

Quantitatively, the dependence between the OH stretching frequencies (ν_{OH}) and the atomic weight and valency of the cations bonded to OH groups can be expressed as:

$$\nu_{OH}(M_2 - M_{2'}) = \left[-1.237(m_{M_2} + m_{M_{2'}}) + 15\left(V_{M_2} + V_{M_{2'}} + \frac{n}{1 + \frac{m_{M_2}}{m_{Al}}} - 4\right) + 3643\right] \text{cm}^{-1} \quad [7]$$

where M_2 and $M_{2'}$ are the cations (Al, Mg, Fe^{3+} and Fe^{2+}) bonded to OH groups; m_{M2}, V_{M2} and $m_{M2'}$, $V_{M2'}$ are the atomic mass and valency of the M_2 and $M_{2'}$ cations, respectively; n is an integer equal to a number of Al cations bonded to OH groups; its value is equal

https://doi.org/10.1346/CCMN.1997.0450205 Published online by Cambridge University Press

to zero (no Al around OH), 1 ($M_{2'}$ = Al) or 2 ($M_{2'}$ = M_2 = Al).

The wave numbers calculated by Equation [7] for all possible M_2-OH-$M_{2'}$ configurations are given in Table 1. The discrepancy between the calculated OH frequencies and those obtained by the mica IR spectra decompositions does not exceed 2 cm^{-1} (Table 1).

A physical meaning for the term:

$$\frac{n}{1 + \frac{m_{M_2}}{m_{Al}}}$$

is not clear. One may assume that Al cations have an "effective" valency higher than +3. Then the value of this term corresponds to a surplus valency of Al, and the "effective" valency of this cation should be equal to 3.25 v.u. for the Al-Fe pairs and 3.5 v.u. for the Al-Mg and Al-Al.

Equation [7] was obtained by analysis of the data presented in Figure 3 using trial and error. It explains the different dependences of the OH frequencies upon the cation valency for cations having similar or different atomic masses. In the first case, the wave numbers will increase because their values depend mainly upon the second term in Equation [7], whereas in the second case, the wave numbers will decrease because the contribution of the first term is higher than second one.

Thus there is an apparent contradiction between the prediction following from the theoretical notions and from Equation [7]. According to the theoretical prediction, a decrease of the total valency of cations bonded to OH groups and having the same mass leads to an increase of the corresponding OH frequency. Equation [7] predicts an opposite effect in accordance with the experimental observations. To explain this contradiction, one has to take into account an interaction between the cations bonded to the OH group and the corresponding proton. An increase in the total cation valency increases the repulsion between the cations and the proton and decreases the interaction OH···03. As a result, the bond strength within the OH group increases, leading to an increase in the OH frequency. Thus, for cations bonded to OH groups, having the same mass but different valency, 2 opposite tendencies overlap: the increase of cation valency decreases the interaction within OH group, but simultaneously a decrease of the OH···03 interaction increases the bond strength within the OH group. The last effect dominates.

Besson and Drits (1997) have found the following set of the relationships between the OH frequencies corresponding to different cationic pairs:

$$2\nu\ (M_2 - M_{2'}) = \nu\ (M_2 - M_2) + \nu\ (M_{2'} - M_{2'}) \quad [8]$$

where M_2 and $M_{2'}$ are the cations differing by their mass and/or valency. For the Fe^{3+}-Fe^{2+}, Fe^{2+}-Mg, Fe^{3+}-Mg, and Al-Mg cationic pairs, Equation [8] follows from Equation [7]. For the Al-Fe^{2+} and Al-Fe^{3+} pairs, a small discrepancy (1–3 cm^{-1}) between the values calculated by Equations [7] and [8] is observed because of the small difference between the values of Al "effective" valency equal to 3.5 v.u. and 3.33 v.u. in Equation [7], which is ignored in Equation [8]. The approach described may be used for prediction of a wave number for a definite cation pair if the wave numbers for the corresponding 2 other bands are known. The approach can be applied only to the same structural type of minerals. For example, the wave number for the Al-Fe^{3+} band corresponding to pyrophyllite-like local cation environments was found using the wave numbers of the Al-Al band in the IR spectra of pyrophyllite and the Fe^{3+}-Fe^{3+} band in the IR spectra of ferripyrophyllite. Figure 3 shows that this wave number should be equal to 3652 cm^{-1}. Decomposition of some of the studied IR spectra has shown the OH band at 3652 cm^{-1} (Tables 1 and 2).

QUANTITATIVE ANALYSIS OF THE OH STRETCHING SPECTRA

The integrated optical density of each band is determined by the number of absorption centers of the given type and by the absorption coefficient. The absorption coefficients for individual bands in the region of OH-stretching vibrations for dioctahedral micas were not determined. However, the mean absorption coefficients for all such bands as well as for V-bands in trioctahedral micas (Rouxhet 1970) have similar values. Slonimskaya et al. (1986) assumed the same value of the absorption coefficient for all individual bands. This assumption can be used as a basis for the determination of the octahedral cation contents. The practical application of the approach is as follows: as each OH group is coordinated by 2 cations, 100% of the integrated optical densities implies 200% of the composition of the octahedral cations:

$$C_{Al} + C_{Fe^{3+}} + C_{Fe^{2+}} + C_{Mg} = 2.0 \quad [9]$$

where C_{Al}, $C_{Fe^{3+}}$, $C_{Fe^{2+}}$ and C_{Mg} are the concentrations of the corresponding cations in the octahedral sheets per structural formula. This implies that the concentration of each octahedral cation (C_i) is equal to the sum of the contribution of the cations to the integrated optical densities W_{ij} of the bands determined by those OH groups that contain the given cation in their nearest environment:

$$C_{Al} = (2W_{Al\text{-}Al})_{cal} + (W_{Al\text{-}Fe^{3+}})_{cal} + (W_{Al\text{-}Mg})_{cal} + (W_{Al\text{-}Fe^{2+}})_{cal} \quad [10]$$

We have used this approach in order to determine the composition of octahedral cations in the samples under study, taking into account the refined correlations between the frequencies and the cation pairs bonded to OH groups, as well as the optical densities

Table 3. Composition of the octahedral cation contents for the samples under study determined by the IR quantitative analysis (I) and from the conventional chemical formulae (II).

	933		132		1040		Z1		69		5/1		655		TAH	
	I	II	I	II	I	II	I	II	I	II	I	II	I	II	I	II
Al	0.00	0.03	0.00	0.04	0.01	0.18	0.05	0.07	0.05	0.08	0.13	0.22	0.16	0.20	0.16	0.34
Fe^{3+}	1.47	1.17	1.32	1.29	1.33	1.19	0.96	0.96	1.15	1.08	1.30	1.22	1.10	1.02	1.07	0.84
Fe^{2+}	0.00	0.27	0.07	0.09	0.27	0.24	0.26	0.27	0.36	0.38	0.07	0.07	0.12	0.15	0.14	0.16
Mg	0.53	0.52	0.57	0.57	0.39	0.39	0.73	0.70	0.41	0.45	0.50	0.48	0.63	0.63	0.64	0.66
	PIL		68/69		E8/2		40/7		CH		136		31		BP	
	I	II	I	II	I	II	I	II	I	II	I	II	I	II	I	II
Al	0.44	0.55	0.55	0.52	0.68	0.66	0.87	0.92	0.92	1.08	1.05	1.04	1.10	1.11	1.11	1.11
Fe^{3+}	0.93	0.84	0.89	0.91	0.79	0.79	0.64	0.57	0.74	0.57	0.17	0.19	0.17	0.21	0.41	0.46
Fe^{2+}	0.21	0.20	0.18	0.19	0.10	0.10	0.20	0.20	0.07	0.08	0.21	0.17	0.07	0.04	0.13	0.08
Mg	0.42	0.40	0.39	0.37	0.43	0.45	0.29	0.31	0.27	0.27	0.59	0.61	0.64	0.64	0.35	0.34
	Z2		MOL		60		RM4		RM30		38/60		BIN			
	I	II	I	II	I	II	I	II	I	II	I	II	I	II		
Al	1.18	1.19	1.27	1.31	1.41	1.40	1.75	1.77	1.86	1.89	2.00	2.00	1.96	1.95		
Fe^{3+}	0.17	0.16	0.05	0.06	0.10	0.07	0.09	0.09	0.00	0.00	0.00	0.00	0.04	0.05		
Fe^{2+}	0.06	0.06	0.00	0.01	0.07	0.08	0.00	0.00	0.00	0.00	0.00	0.00	0.00	0.00		
Mg	0.57	0.59	0.68	0.63	0.42	0.45	0.15	0.15	0.14	0.11	0.00	0.00	0.00	0.00		

of the cation pairs (Table 2). In addition, we have taken into consideration that IR spectra of Al-Fe^{3+} micas having a deficiency of interlayer K contain OH bands corresponding to local pyrophyllite-like environments. Table 2 shows the values of integrated optical densities of the Al-Al, Al-Fe, and Fe-Fe bands corresponding to such environments. Table 3 compares the octahedral cation compositions determined from the crystal chemical formulae with those calculated by Equations similar to [9] using the data of Table 2. The differences between the 2 values, that is, the values $[C_{IR} - C_{Chem}]$, are usually less than 0.03 a.u. per half unit cell: i.e., the errors do not exceed 2%. Table 3 shows that all samples can be divided into 2 main groups. The first group includes samples (132, Z1, 69, 68/69, E8/2, 31, BP, Z2, E8/2, MOL, 60, RM4, RM30, 136, BIN), for which octahedral cation contents determined by chemical analysis and IR spectra decomposition coincide within the errors for all 4 cation types.

The second group of samples (933, 1040, 5/1, 655, TAH, PIL, 40/7, CH) provides examples of the more complex IR spectra for which a distinct discrepancy between the distribution of the optical densities at low and high frequencies and the proportions of Fe^{3+} and Al in the crystallochemical formulae has been observed (Tables 2 and 3). The IR spectrum of the sample 1040 is demonstrative in this respect. According to the conventional structural formula of this sample (Table 3), the octahedra contain no Al, whereas the IR spectrum contains the Al-Mg band at 3605 cm^{-1} of considerable intensity (Table 2).

There are 3 important features of the samples of the second group (Table 3): 1) The contents of Mg and Fe^{2+} determined by the IR spectra decomposition and the chemical analysis have the same values within error. 2) The total amount of Fe^{3+} and Fe^{2+} cations determined by both methods also coincide. 3) For each sample, the difference between the amount of the Al cations determined from the IR spectra and conventional crystallochemical formulae are within an error equal to the difference between the amount of Fe^{3+} cations determined from chemical analysis and the IR spectrum:

$$(C_{Al})_{Chem} - (C_{Al})_{IR} \cong (C_{Fe^{3+}})_{IR} - (C_{Fe^{3+}})_{Chem} \qquad [11]$$

Taking into account these data, the discrepancy may be due to the fact that, according to the conventional method of calculation of crystallochemical formula, Si is replaced first of all by Al and then by Fe^{3+} only when Al is lacking. As Slonimskaya et al. (1986) noted, this may not always be correct. Equation [11] may imply that the amount of Fe^{3+} corresponding to the difference between $(C_{Fe^{3+}})_{Chem}$ and $(C_{Fe^{3+}})_{IR}$ should be placed in tetrahedral positions instead of the same amount of Al which then should be placed in octahedral sites. The corrected crystallochemical formulae of the samples of the second group are presented in Table 4. This approach eliminates the discrepancy in the data obtained from the conventional crystallochemical formulae and the IR spectra decomposition without changing the total chemical composition of each sample. The difference between the octahedral cation contents in the revised formulae and those obtained from the IR spectra did not exceed 0.04 a.u. per half unit cell for the samples of the first group.

The results show that this technique of determining the octahedral cation content simultaneously permits refinement of the composition of the tetrahedral cations. In some cases, this approach may correct chemical analysis data that are in error due to Fe^{2+} oxida-

https://doi.org/10.1346/CCMN.1997.0450205 Published online by Cambridge University Press

Table 4. The refined distribution of isomorphous cations among octahedral and tetrahedral positions in the Al-Fe^{3+}-containing mica samples: (I) according to the conventional chemical formula; (II) according to decomposition of IR spectra; (III) according to the revised chemical formulae.

	933			132			1040			5/1			655		
	I	II	III	I	II	III	I	II	III	I	II	III	I	II	III
Tet															
Si	3.88		3.88	3.96		3.96	3.79		3.79	3.69		3.69	3.71		3.71
Al	0.02		0.00	0.04		0.00	0.21		0.07	0.31		0.22	0.29		0.24
Fe^{3+}	0.10		0.12	0.00		0.04	0.00		0.14	0.00		0.09	0.00		0.05
Oct															
Al	0.00	0.03	0.03	0.00	0.04	0.04	0.01	0.18	0.16	0.13	0.22	0.22	0.16	0.20	0.20
Fe^{3+}	1.47	1.17	1.17	1.32	1.29	1.30	1.33	1.19	1.20	1.30	1.22	1.22	1.10	1.02	1.02
Fe^{2+}	0.00	0.27	0.27	0.07	0.09	0.09	0.27	0.24	0.24	0.07	0.07	0.07	0.12	0.15	0.15
Mg	0.53	0.52	0.53	0.57	0.57	0.57	0.39	0.39	0.39	0.50	0.48	0.48	0.63	0.63	0.63
	TAH			PIL			40/7			CH					
	I	II	III	I	II	III	I	II	III	I	II	III			
Tet															
Si	3.72		3.72	3.73		3.73	3.70		3.70	3.42		3.42			
Al	0.28		0.07	0.27		0.17	0.30		0.25	0.58		0.41			
Fe^{3+}	0.00		0.21	0.00		0.10	0.00		0.05	0.00		0.17			
Oct															
Al	0.16	0.34	0.34	0.44	0.55	0.55	0.87	0.92	0.92	0.92	1.08	1.08			
Fe^{3+}	1.07	0.84	0.84	0.93	0.84	0.85	0.64	0.57	0.57	0.74	0.57	0.57			
Fe^{2+}	0.14	0.16	0.16	0.21	0.20	0.20	0.20	0.20	0.20	0.07	0.08	0.08			
Mg	0.64	0.66	0.66	0.42	0.40	0.40	0.29	0.31	0.31	0.27	0.27	0.27			

tion. For example, according to the IR data the sample 933 contains 0.28 cations of Fe^{2+} per half-unit cell, whereas chemical analysis found only Fe^{3+} cations in the sample. However, the total amount of Fe cations determined from the IR spectrum is 1.45 a.u. and the chemical analysis is 1.47 a.u. per unit formula.

DISCUSSION

Analysis of the factors controlling the positions of the OH bands has allowed us to identify each band presented in the IR spectra of the mica samples containing Al, Mg, Fe^{3+} and Fe^{2+} cations in octahedra, and Si, Al and Fe^{3+} cations in tetrahedra of 2:1 layers. Among the factors responsible for the band frequencies, the most important are the valency and atomic weight of cations bonded to OH groups. For this reason, the position of the band corresponding to a defined cation pair reveals only a small dependence upon the chemical composition of the sample (Besson and Drits 1997).

An elementary explanation of the observed regularities is the assumption that an increase in mass of cations bonded to OH groups increases the reduced mass of the OH vibration system and decreases the frequency. Another dominant factor affecting the OH stretching frequencies is the bond strength within hydroxyl groups, which is in turn controlled to some degree by the OH···O_3 hydrogen bonding. The simple relationships between atomic weights and valencies of the cations bonded to OH groups and wave numbers of the corresponding bands support the validity of these assumptions. One may expect that the relationships similar to Equations [7] and [8] are valid for other phyllosilicates. The predictive nature of such relationships shows their practical significance.

Determinations of OH vector orientations in different local cation environments around OH groups, O_3 and O_1 atoms in mica structures having different chemical compositions, are absent. However, the role of this factor may be estimated using the determinations of the OH vector orientation by electrostatic calculations and single crystal structural refinements. For example, let us compare the wave numbers of the Al-Al bands for dickite, kaolinite and pyrophyllite. To a first approximation, the inner OH group in the structure of these minerals has the same local environment, because the tetrahedral sheets contain only Si and the octahedral sheets only Al. However, the Al-Al band frequencies corresponding to the inner OH groups are equal to 3675 cm^{-1} for pyrophyllite and to 3620 cm^{-1} for kaolinite and dickite (Farmer 1974). According to Joswig and Drits (1986) and Bish (1993), the OH vectors in dickite and kaolinite structures form with the (001) plane angle close to 1°, whereas in pyrophyllite this angle is equal to 26° (Evans and Guggenheim 1988). The reason for different ρ angles is connected to the features of the actual crystal structures of these minerals (Rozdestvenskaya et al. 1982; Bookin and Drits 1982; Evans and Guggenheim 1988). The essential point is that the small ρ angle in dickite and kaolinite provides stronger OH···O_3 hydrogen bonding and a lower frequency for the inner OH group than for those in pyrophyllite.

https://doi.org/10.1346/CCMN.1997.0450205 Published online by Cambridge University Press

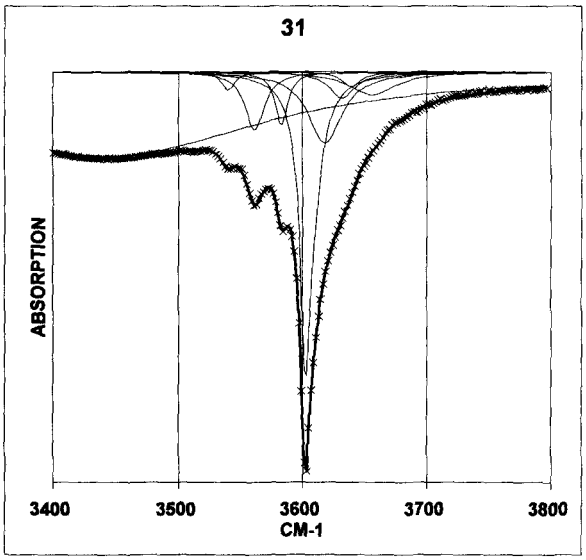

Figure 4. Decomposition of the IR spectrum of sample 31, having the structural formula: $K_{0.81}Na_{0.03}(Al_{1.10}Fe_{0.17}Fe_{0.07}Mg_{0.64})(Si_{3.94}\ Al_{0.06})O_{10}(OH)_2$.

A strong influence of the OH vector orientation on the vibration of OH groups bonded to a certain cation pair is demonstrated by the comparison of the Fe^{3+}-Fe^{3+} band positions in the IR spectra of celadonite (3534 cm^{-1}) and ferripyrophyllite (3631 cm^{-1}). In both minerals, tetrahedral sites are occupied by Si, but in the celadonite structure there are additional electrostatic interactions between protons of OH groups and interlayer K cations. The absence of K interlayer cations in ferripyrophyllite eliminates this interaction and increases the inclination of the OH vector with respect to the (001) plane. For this reason, in celadonite the interaction between protons of the OH groups and the O_3 atoms is stronger than that in ferripyrophyllite. As a result, a difference between wave numbers of the Fe^{3+}-Fe^{3+} bands corresponding to ferripyrophyllite and celadonite is about 97 cm^{-1}. The validity of these considerations is further supported by calculations of the OH vector orientation for 2 different local environments in the dehydrated structure of K-nontronite (Dainyak et al. 1984). For this mineral, the ρ angle increases from 23° for the [$2Fe^{3+}$] [4Si] [2K] environment around the OH group, to 62° for the [$2Fe^{3+}$ [4Si] (2ù], where ù signifies an interlayer vacancy. Thus the 25° and 39° differences in the ρ angles correspond to the 55 and 97 cm^{-1} differences in the frequencies of the Al-Al and Fe^{3+}-Fe^{3+} bands, respectively. On average, changing the ρ angle by 1° may change the band frequency by up to 2.5 cm^{-1}. We conclude that, for each given cation pair bonded to an OH group, the OH-vibration depends upon the OH···O_3 hydrogen bonding which, in turn, depends upon the OH vector orientation.

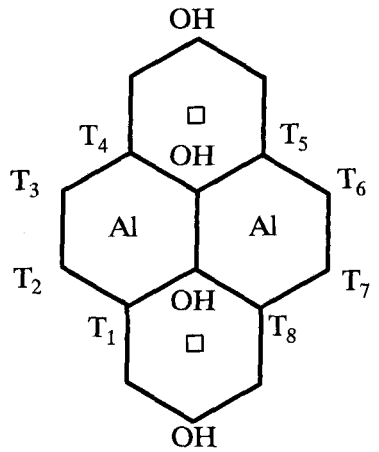

Figure 5. The distribution of tetrahedral cations T_i (i = 1–8) around the Al-OH-Al configuration.

The observed low sensitivity of the OH stretching band positions to the mica sample chemical composition, in combination with wide variations of the band widths, allows the assumption that, for each defined pair of cations bonded to OH groups, different local cation environments only slightly change the OH vector orientations leading to band broadening. It is interesting to compare the features of the IR spectra for samples having homogeneous cation composition in either tetrahedral or octahedral sheets. Celadonites and leucophyllite, having a minimal substitution of Al for Si in tetrahedra, are characterized by IR spectra containing a set of well-resolved absorption peaks (Figure 4). The smallest width of bands usually corresponds to the R^{3+}-R^{2+} pairs, probably due to the ordered distribution of hetero-valent cations within the structure of these samples. Note that the well-resolved absorption peaks in the IR spectra of these samples are observed at frequencies lower than 3610 cm^{-1}. In other words, the region of the OH vibrations corresponding to the Al-Al bands is always represented by smooth curves that show a gradual decrease in absorption with increasing frequencies.

Fe- and Mg-free illites and muscovites, in spite of the homogeneous octahedral cation content, are characterized by very broad and poorly resolved maxima in the OH stretching vibration region. The main reason is the partial overlapping of the Al-Al bands having distinct frequencies. The presence of several Al-Al bands in the illite IR spectra may be related to the different numbers of Al^{IV} cations close to OH groups. Figure 5 shows that there are 8 tetrahedral sites close to the OH group that can contain different amounts of Si and Al^{IV}. In particular, the number of Si cations can change from 8 to 4. The OH vector orientation will depend upon the amount and distribution of Al^{IV} cations over these sites; the greater number of Al^{IV} cations, the greater the ρ angle (Bookin and Drits 1982).

https://doi.org/10.1346/CCMN.1997.0450205 Published online by Cambridge University Press

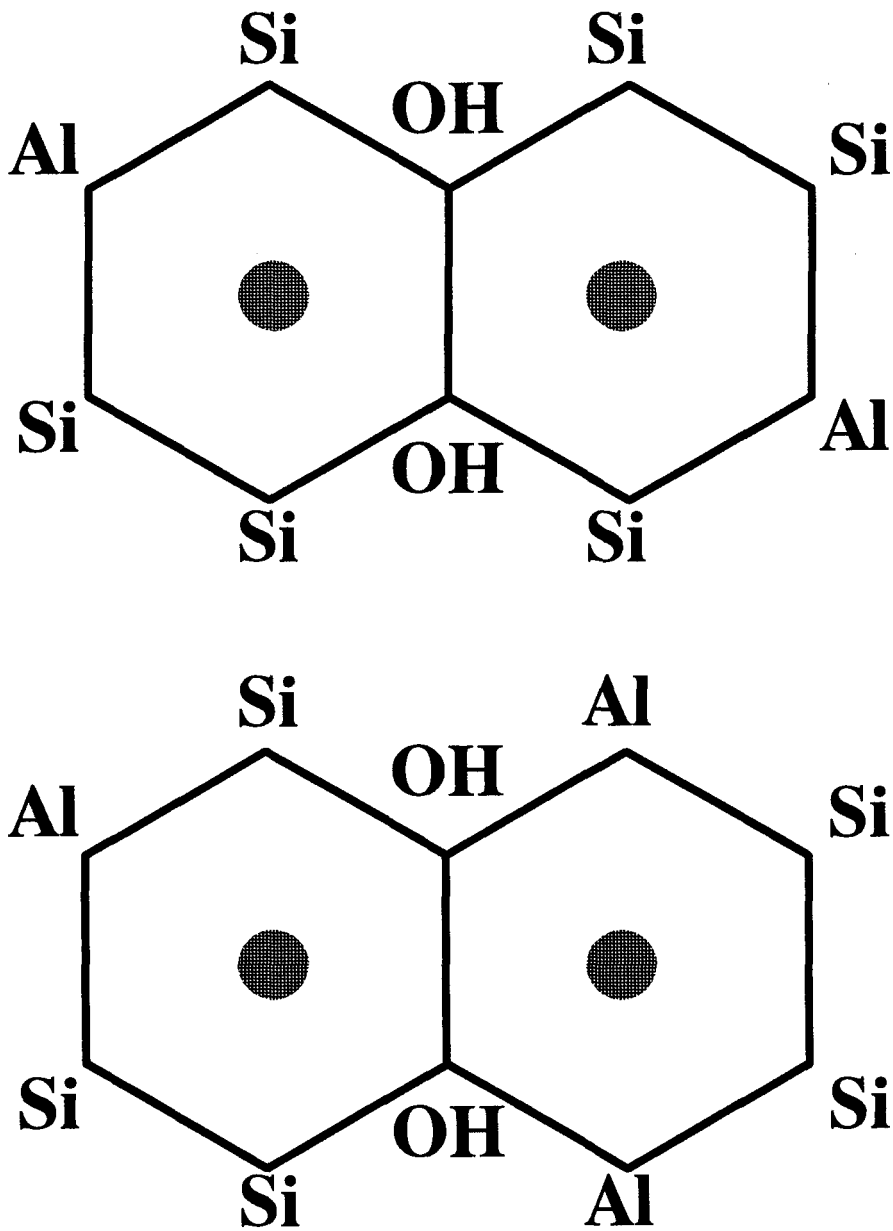

Figure 6. Two different possible distributions of tetrahedral Si and Al cations around the M_2-OH-M_2 configuration.

As a result, an increase in the number of Al^{IV} cations around OH groups should decrease the OH···O_3 interaction and increase the OH stretching frequency.

The 3 distinct Al-Al bands extracted from the IR spectra of illites and muscovites (samples: RM4, RM30, 38/60, Table 2) probably correspond to local structural fragments containing 7–8, 6–7, and 4–5 cations of Si, respectively, among the 8 tetrahedral sites. In this case, the width of these bands should depend upon the distribution of Al^{IV} over the available 8 sites. This means that, in general, the IR spectrum of muscovite may be decomposed into a large number of Al-Al bands having slightly different frequencies.

The data in Table 2 show that, in the IR spectra of the leucophyllite-like samples (136, 31, MOL), the Al-Al band has the lowest frequency (near 3620 cm^{-1}) and the highest optical density. The other 2 Al-Al bands have a significantly lower absorption intensity. The appearance of Al-Al bands that have approximately the same frequencies in all studied illite-muscovite IR spectra can be considered evidence for the similarity of the local environments around Al-OH-Al

https://doi.org/10.1346/CCMN.1997.0450205 Published online by Cambridge University Press

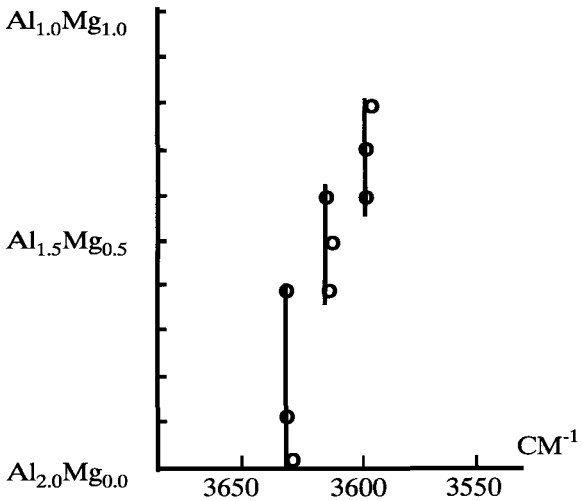

Figure 7. The dependence between the positions of the major intensity OH bands and the octahedral cation compositions of the dioctahedral Al-Mg micas (modified after Velde 1978).

configurations in these minerals. The Al-Al band at 3620 cm^{-1} should correspond to the local cation environment containing 8 Si atoms nearest to the Al-Al pair. Figure 6 shows several local environments of tetrahedral cations around Al-OH-Al that should change the OH vector orientation and lead to shifting and broadening of the Al-Al bands.

If this interpretation is valid, we need an answer for the question of why several bands with distinct frequencies are observed only for Al-Al pairs. We have studied samples having similar amounts of Al^{VI} and Fe^{3+} and a high content of Al^{IV} (samples 68/69, 40/7, CH, E8/2). However, the decomposition of their IR spectra always requires at least 2 Al-Al and only 1 Fe^{3+}-Fe^{3+} band. One has to emphasize that the position and the number of these bands have been determined from the IR spectra of celadonite and muscovite. Note that the OH stretching vibration region of the pyrophyllite IR spectrum consists of a single Al-OH-Al band (Farmer 1974; Besson and Drits 1997).

One possible explanation is that, in the samples under study, all types of cation pairs except Al-Al have similar local cation environments, and, as a result, similar orientations of the OH vectors for each given cation pair. If this supposition is valid, it must be assumed that the samples under study consist of at least 2 main local domains having different composition and distribution of isomorphous cations. One of them may have illite-like and the other, leucophyllite- or celadonite-like composition. The strong tendency to the ordered distribution of hetero-valent octahedral cations in combination with the minimum content of Al^{IV} in the latter type of domains may explain similar local environments around each given cation pair. The presence of illite-like domains may explain the appearance of the Al-Al bands having distinct frequencies. The existence of celadonite-like and illite-like small domains in Al containing glauconites was assumed on the basis of the interpretation of Mössbauer spectra of these samples (Daynyak and Drits 1987; Dainyak et al. 1992).

Our model can be used to explain the dependence between the major intensity band positions and $Al_t = Al^{IV} + Al^{VI}$ proposed by Robert and Kodama (1988) for Al-Mg dioctahedral micas. To make it clear, let us consider the data obtained by Velde (1978) for the muscovite-leucophyllite series of samples. Figure 7 shows how the positions of the major intensity band depend upon the sample chemical composition. In the spectra of the samples containing 60, 70 and 80 percent leucophyllite, the main absorption maximum at 3600 cm^{-1} corresponds to the Al-Mg band. This means that the Al-Mg cationic pairs bonded to OH groups prevail due to the ordered distribution of Al and Mg. However, according to Equation [6] the positions of the major intensity band should be at 3608, 3610 and 3613 cm^{-1} for the samples containing, respectively, 80, 70 and 60 percent of leucophyllite component. The discrepancy between the observed and predicted frequencies is probably due to number of the Al-OH-Al configurations in these samples not being sufficient to shift the main absorption maximum. Vibrations of the OH groups bonded to Al cause the asymmetrical profile of the absorption maxima on the higher frequency side.

The position of the major intensity band at 3630 cm^{-1} in the IR spectra of muscovite (Figure 7) reflects the overlapping of the Al-Al bands at frequencies of 3620 and 3641 cm^{-1}. The contribution from the third Al-Al band appears as a shoulder at the higher frequency side of the spectrum. These features are observed in the muscovite IR spectrum shown in Figure 8. The sample containing equal amounts of muscovite and leucophyllite components contains equal proportions of Al-Mg and Al-Al pairs bonded to OH groups. The adsorption maximum in the IR spectrum of this sample corresponds to a wave number equal to 3610 cm^{-1}. It is natural to assume that the absorption maximum results from the overlapping of the Mg-Al band at 3600 cm^{-1} and the Al-Al band at 3620 cm^{-1} (Figure 9).

As mentioned earlier, some illite and glauconite samples contain bands whose frequencies correspond to the Al-Al bands in the IR spectra of pyrophyllite and the Fe^{3+}-Fe^{3+} bands in the IR spectra of ferripyrophyllite. This means that micaceous minerals having a deficiency of K cations in interlayers contain pyrophyllite-like domains of different octahedral cation contents: Al-Al, Al-Fe^{3+} and Fe^{3+}-Fe^{3+}. We do not know in what forms pyrophyllite-like structural fragments are present in illite and glauconite samples. These fragments may occur as local domains within

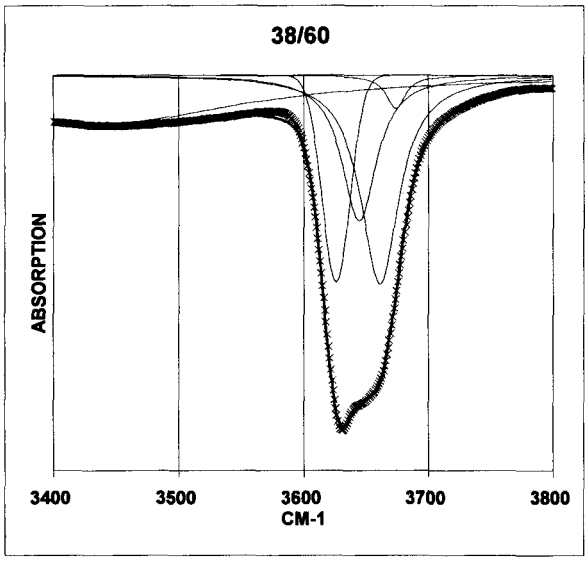

Figure 8. The IR spectrum within the OH stretching frequency region for the synthetic muscovite sample 38/60 having the composition $K_{0.79}Na_{0.03}Al_{2.00}$ $(Si_{3.18}Al_{0.82})O_{10}(OH)_2$.

the same layers or as alternate mica and pyrophyllite layers. The presence of individual pyrophyllite layers within an illite matrix has been observed by high-resolution transmission electron microscopy (HRTEM) for one of the studied samples (Tsipursky, personal communication 1993).

Satisfactory agreement between the octahedral cation contents determined from the IR spectra and the chemical analysis has shown that the integrated optical densities can be used for the study of the local order-disorder in the isomorphous cation distribution. However, the identification of the individual bands requires certain caution. The problem arises because of the close positions of some bands corresponding to different cation configurations. For example, the Al-Fe^{2+} and Mg-Fe^{3+} bands have practically the same frequencies (Table 1). For some samples, the Al-Al band at 3658 cm^{-1} may overlap with the Al-Fe^{3+} band at 3652 cm^{-1}, corresponding to the pyrophyllite local environment. Under these circumstances, the best way to determine the short-range cation ordering in micaceous minerals consists of the decomposition of IR spectra of samples having a known chemical composition.

The possibility that Fe^{3+} cations replace Si in the presence of Al in tetrahedral sheets of phyllosilicates has been discussed by many researchers (Slonimskaya et al. 1986; Besson et al. 1983; Cardile 1989). Until now the solution of this problem has met with methodological difficulties. One of the essential consequences of the quantitative analysis of the IR spectra is the determination of the tetrahedral Fe^{3+} cations in the structure of some studied samples. This result shows that a conventional presentation of chemical formulae for Al-Fe^{3+} containing 2:1 layer silicates is unacceptable without consideration of Fe^{3+} in the tetrahedral layer.

ACKNOWLEDGMENTS

We thank E. Silvester, D.D. Eberl and P. Eberl for the English corrections. V. A. Drits thanks the Orléans University (France) and the Russian SF for financial support of this work (grant 95-05-14509). Source of Tsipursky 1993 personal com-

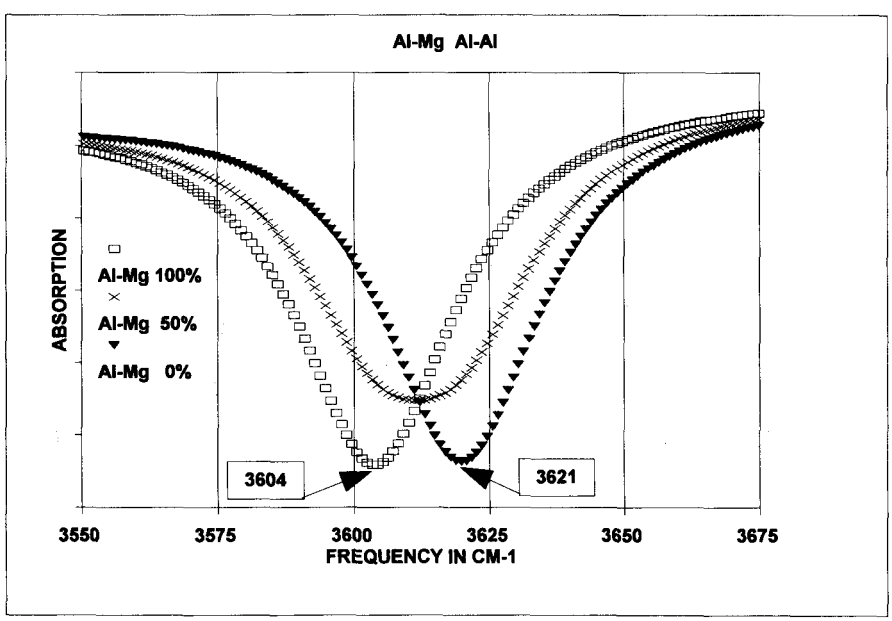

Figure 9. A superposition of the Al-Mg and Al-Al bands whose wave numbers are equal to 3621 and 3604 cm^{-1}, respectively.

munication: S. I. Tsipursky, American Colloid Company, Arlington Heights, Illinois 60004-1440.

REFERENCES

Besson G, Bookin AS, Dainyak LG, Tchoubar C, Drits VA. 1983. Use of diffraction and Mössbauer methods for the structural and crystallochemical character cation in nontronite. J Appl Crystallogr 16:374–382.

Besson G, Drits VA. 1997. Refined relationships between chemical composition of dioctahedral fine-grained micaceous minerals and their infrared spectra within the OH stretching region. Part 1: Identification of the OH stretching bands. Clays Clay Miner 45:158–169.

Bish DL. 1993. Rietveld refinement of the kaolinite structure at 1.5K. Clays Clay Miner 41:738–744.

Bookin AS, Drits VA. 1982. Factors affecting orientation of OH vector in mica. Clays Clay Miner 30:415–421.

Bookin AS, Smoliar BB. 1985. Simulation of bond lengths in coordination polyhedra of 2:1 layer silicates. In: Konta J, editor. The 5th Meeting of the European Clay Groups. Prague: Universita Karlovo. p 51–56.

Brindley GW, Kao CC. 1984. Structural and IR relations among brucite-like divalent metal hydroxides. Phys Chem Miner 10:187–191.

Cardile CM. 1989. Tetrahedral iron in smectite: a critical comment. Clays Clay Miner 37:185–188.

Cardile CM, Brown IWM. 1988. An ^{57}Fe Mössbauer spectroscopic and X-ray diffraction study of New Zealand Glauconites. Clay Miner 23:13–25.

Dainyak LG, Bookin AS, Drits VA. 1984. Interpretation of the Mössbauer spectra of dioctahedral Fe^{3+} layer silicates. Part III—Celadonite. Kristallographiya 29:312–321 (in Russian).

Daynyak LG, Drits VA. 1987. Interpretation of Mössbauer spectra of nontronite, celadonite and glauconite. Clays Clay Miner 35:363–372.

Dainyak LG, Drits VA, Heifits LM. 1992. Computer simulation of cation distribution in dioctahedral 2:1 layer silicates using IR-data: Application to Mössbauer spectroscopy of a glauconite sample. Clays Clay Miner 40:470–479.

Evans BW, Guggenheim S. 1988. Talc, pyrophyllite and related minerals. In: Bailey SW, editor. Hydrous phyllosilicates (exclusive of mica). Rev Mineral 19:225–280.

Farmer VC. 1974. The layer silicates. In: Farmer VC, editor. The infrared spectra of minerals. London: Mineral Soc. p 331–364.

Giese RF. 1979. Hydroxyl orientations in 2:1 phillosilicates. Clays Clay Miner 27:213–223.

Johnston JH, Cardile CM. 1987. Iron substitution in montmorillonite and glauconite by ^{57}Fe Mössbauer spectroscopy. Clays Clay Miner 35:170–171.

Joswig W, Drits VA. 1986. The orientation of the hydroxyl groups in dickite by X-ray diffraction. N Jb Miner Abh 147:19–22.

Langer K, Chatterjee ND, Abraham K. 1981. Infrared studies of some synthetic and natural $2M_1$ dioctahedral micas. N Jb Miner Abh 142:91–110.

Robert JL, Kodama H. 1988. Generalization of the correlation between hydroxyl-stretching wavenumbers and composition of micas in the system K_2O-M_2O-Al_2O_3-SiO_2-H_2O: A single model for trioctahedral and dioctahedral micas. Am J Sci 228A:196–212.

Rouxhet PG. 1970. Hydroxyl stretching bands in micas: A quantitative interpretation. Clay Miner 8:375–388.

Rozdestvenskaya IV, Drits VA, Bookin AS, Finko VI. 1982. Location of protons and structural peculiarities of dickite mineral. Mineralogichesky Zhurnal 4:52–58 (in Russian).

Saksena BD. 1964. Infrared hydroxyl frequencies of muscovite, phlogopite and biotite micas in relation to their structures. J Chem Soc, Faraday Trans 60:1715–1725.

Slonimskaya MV, Besson G, Dainyak LG, Tchoubar C, Drits VA. 1986. Interpretation of the IR spectra of celadonites, glauconites in the region of OH stretching frequencies. Clay Miner 21:377–388.

Smoliar BB, Drits VA. 1990. Structural modelling micas having disordered distribution of isomorphous cations. Mineralogichesky Zhurnal 10:68–72 (in Russian).

Vedder W. 1964. Correlations between infrared spectrum and chemical composition of mica. Am Mineral 49:736–768.

Velde B. 1978. Infrared spectra of synthetic micas in the muscovite Mg-Al celadonite. Am Mineral 63:343–349.

Velde B. 1983. Infrared OH-stretch bands in pottasic micas, talc, and saponite; influence of electronic configuration and site of charge compensation. Am Mineral 68:1169–1173.

Wilkins RWT, Ito J. 1967. Infrared spectra of some synthetic talcs. Am Mineral 52:1649–1661.

(Received 19 June 1995; accepted 26 April 1996; Ms. 2661, Part II)